arXiv:hep-ex/0102043 22 Feb 2001

LC-PHSM-2001-020
February 20, 2001

Measurement of the leptoquark Yukawa couplings in e^+e^- collisions at TESLA

Aleksander Filip Żarnecki
Institute of Experimental Physics, Warsaw University,
Hoża 69, 00-681 Warszawa, Poland
E-mail: zarnecki@fuw.edu.pl

Abstract

Measurement of the Yukawa couplings of the first-generation leptoquarks has been studied for e^+e^- collisions at TESLA, at $\sqrt{s}$ =800 GeV. By combining measurements from different production and decay channels, determination of Yukawa couplings with precision on the few per-cent level is possible. TESLA will be sensitive to very small leptoquark Yukawa couplings not accessible at LHC, down to $\lambda_{L,R} \sim 0.05e$. Distinction between left-handed and right-handed Yukawa couplings is feasible even for leptoquark masses very close to the pair-production kinematic limit.

1 Introduction

New result on atomic parity violation (APV) in Cesium and unitarity of the CKM matrix, as well as recent LEP2 hadronic cross-section measurements indicate possible deviations from the Standard Model predictions. Exchange of leptoquark type objects with masses above 250GeV has been proposed as a possible explanation for these effects [1]. If the leptoquark Yukawa couplings are assumed to be small, leptoquark masses of the order of 300 GeV are consistent with the exiting data.

Running at high luminosity LHC experiments will search for leptoquark pair production for leptoquark masses up to about 1.5 TeV [2, 3]. Leptoquark mass can be determined at LHC with high precision, limited mainly by the systematic uncertainty of the energy scale. However, leptoquark pair production in strong interactions is not sensitive to the leptoquark Yukawa couplings. Yukawa couplings could be measured in the Drell-Yan process at LHC for coupling to the mass ratios λ/M down to about 0.1 TeV^{-1} [3]. However, the measurement is only possible if the leptoquark type (spin, corresponding quark flavor,

coupling chirality) is known.[1] The value of the leptoquark pair production cross-section and the leptoquark branching fractions will allow differentiation between some leptoquark models at LHC. But the precise determination of the leptoquark type may not be possible.

For masses below 400 GeV leptoquarks can be also pair produced in e^+e^- collisions at TESLA, at $\sqrt{s} = 800$ GeV. The value of the total cross-section and the angular distribution of the produced leptoquark pairs depend on the leptoquark type and the leptoquark Yukawa couplings. Also the single leptoquark production can be used to constrain leptoquark parameters.

In this note, precision with which leptoquark Yukawa couplings can be determined at TESLA is studied. The leptoquark models used in this analysis are described in section 2. Results from the global analysis of available experimental data [1] and the possible leptoquark signal are briefly summarized in section 3. Leptoquark production at TESLA is described in section 4 and the event selection methods in section 5. Yukawa coupling determination from the observed angular distributions is described in section 6.

2 Leptoquark models

In this paper a general classification of leptoquark states proposed by Buchmüller, Rückl and Wyler [4] will be used. The Buchmüller-Rückl-Wyler (BRW) model is based on the assumption that new interactions should respect the $SU(3)_C \times SU(2)_L \times U(1)_Y$ symmetry of the Standard Model. In addition leptoquark couplings are assumed to be family diagonal (to avoid FCNC processes) and to conserve lepton and baryon numbers (to avoid rapid proton decay). With all these assumptions there are 10 possible states (isospin singlets or multiplets) of scalar and vector leptoquarks. Table 1 lists these states according to the so-called Aachen notation [5]. An S(V) denotes a scalar(vector) leptoquark and the subscript denotes the weak isospin. A tilde is introduced to differentiate between leptoquarks with different hypercharges. Listed in Table 1 are the leptoquark fermion number F, electric charge Q, and the branching ratio to an electron-quark pair (or electron-antiquark pair), β. For a given electron-quark branching ratio β, the branching ratio to the neutrino-quark is by definition $(1-\beta)$. Also included in Table 1 are leptoquark-electron-quark couplings, in units of the Yukawa couplings λ_L and λ_R, and the flavors of the lepton-quark pairs coupling to a given leptoquark type. Strong bounds from rare decays [4, 6] indicate that leptoquarks couple only either to left- or to right-handed leptons, i.e. $\lambda_L \cdot \lambda_R = 0$. With this additional constraint, four leptoquark models ($S_\circ$, $S_{1/2}$, $V_\circ$ and $V_{1/2}$) have to be considered separately for left- and right-handed couplings (assuming $\lambda_R = 0$ and $\lambda_L = 0$ respectively). In that case, an additional superscript indicates the coupling chirality. Present analysis takes into account only leptoquarks which couple to the first-generation leptons (e, ν_e) and first-generation quarks (u, d), as they can be best studied at TESLA.

[1] For different leptoquark models contribution to the Drell-Yan lepton pair production cross-section can differ even by an order of magnitude.

Model	Fermion number F	Charge Q	$BR(LQ \to e^{\pm}q)$ β	LQ-e-q Coupling	Channel	
$S_\circ$	2	$-1/3$	$\frac{1+r}{2+r}$	λ_L	eu	νd
				λ_R	eu	
$\tilde{S}_\circ$	2	$-4/3$	1	λ_R	ed	
$S_{1/2}$	0	$-5/3$	1	λ_L	$e\bar{u}$	
				λ_R	$e\bar{u}$	
		$-2/3$	$\frac{1}{1+r}$	λ_L		$\nu\bar{u}$
				λ_R	$e\bar{d}$	
$\tilde{S}_{1/2}$	0	$-2/3$	1	λ_L	$e\bar{d}$	
		$+1/3$	0	λ_L		$\nu\bar{d}$
S_1	2	$-4/3$	1	$\sqrt{2}\lambda_L$	ed	
		$-1/3$	1/2	λ_L	eu	νd
		$+2/3$	0	$\sqrt{2}\lambda_L$		νu
$V_\circ$	0	$-2/3$	$\frac{1+r}{2+r}$	λ_L	$e\bar{d}$	$\nu\bar{u}$
				λ_R	$e\bar{d}$	
$\tilde{V}_\circ$	0	$-5/3$	1	λ_R	$e\bar{u}$	
$V_{1/2}$	2	$-4/3$	1	λ_L	ed	
				λ_R	ed	
		$-1/3$	$\frac{1}{1+r}$	λ_L		νd
				λ_R	eu	
$\tilde{V}_{1/2}$	2	$-1/3$	1	λ_L	eu	
		$+2/3$	0	λ_L		νu
V_1	0	$-5/3$	1	$\sqrt{2}\lambda_L$	$e\bar{u}$	
		$-2/3$	1/2	λ_L	$e\bar{d}$	$\nu\bar{u}$
		$+1/3$	0	$\sqrt{2}\lambda_L$		$\nu\bar{d}$

Table 1: A general classification of leptoquark states in the Buchmüller-Rückl-Wyler model. Listed are the leptoquark fermion number, F, electric charge, Q (in units of elementary charge), the branching ratio to electron-quark (or electron-antiquark), β, leptoquark-electron-quark couplings in terms of the Yukawa couplings λ_L and λ_R, and the flavors of the coupled lepton-quark pairs. For $S_\circ$, ${}^{-2/3}S_{1/2}$, $V_\circ$ and ${}^{-1/3}V_{1/2}$ leptoquarks, the branching ratio β depends on the coupling ratio $r = \lambda_R^2/\lambda_L^2$.

Second- and third-generation leptoquarks as well as generation-mixing leptoquarks will not be considered in this paper. It is also assumed that one of the leptoquark types gives the dominant contribution, as compared with other leptoquark states and that the interference between different leptoquark states can be neglected. Using this simplifying assumption, different leptoquark types can be considered separately. Finally, it is assumed that different leptoquark states within isospin doublets and triplets have the same mass.

3 Current limits from global analysis

In a recent paper[1] available data from HERA, LEP and the Tevatron, as well as from low energy experiments are used to constrain the Yukawa couplings λ and masses M for scalar and vector leptoquarks. To compare the data with predictions of the BRW model the global probability function $\mathcal{P}(\lambda, M)$ is introduced, describing the probability that the data come from the model described by parameters λ and M. The probability function is defined in such a way that the Standard Model probability $\mathcal{P}_{SM} \equiv 1$. Constraints on the leptoquark couplings and masses were studied in the limit of very high leptoquark masses (using the contact interaction approximation [7]) as well as for finite leptoquark masses, with mass effects correctly taken into account. Excluded on 95% confidence level are all models (parameter values) which result in the global probability less than 5% of the Standard Model probability: $\mathcal{P}(\lambda, M) < 0.05$. For models which describe the data much better than the Standard Model ($\mathcal{P}_{max} \equiv \max_{\lambda,M} \mathcal{P}(\lambda, M) \gg 1$) the 95% CL signal limit is defined by the condition: $\mathcal{P}(\lambda, M) > 0.05 \cdot \mathcal{P}_{max}$.

Current limits on the leptoquark masses are mainly based on the negative search results at the Tevatron. For scalar leptoquark models considered in this paper 95% CL exclusion limits on the leptoquark masses are between 213 and 245 GeV. Data sensitive to the virtual leptoquark exchange result in limits on the leptoquark mass M to the Yukawa coupling λ. 95% CL exclusion limits on M/λ, obtained from the global analysis of existing data, range for the scalar leptoquarks from about 2 to 4 TeV. Assuming leptoquark mass of 350 GeV, this corresponds to the limits on the scalar leptoquark Yukawa coupling between 0.09 and 0.17 ($0.27e$ to $0.53e$; $e = \sqrt{4\pi\alpha_{em}}$).

Four leptoquark models are found to describe the existing experimental data much better than the Standard Model ($\mathcal{P}(\lambda, M) > 20$). The signal limits for these models, at 68% and 95% CL are compared with exclusion limits in the (λ, M) space in Figure 1. For S_1 and $\tilde{V}_\circ$ leptoquarks the observed increase in the global probability by factor 367 and 142 respectively corresponds to more than a 3σ effect. The leptoquark "signal" is mostly resulting from the new data on the atomic parity violation (APV) in cesium[8]. After the theoretical uncertainties have been significantly reduced, the measured value of the cesium weak charge is now 2.5σ away from the Standard Model prediction. Also the new hadronic cross-section measurements at LEP2, for $\sqrt{s}$=192–202 GeV, are on average about 2.5% above the predictions[9]. The effect is furthermore supported by the

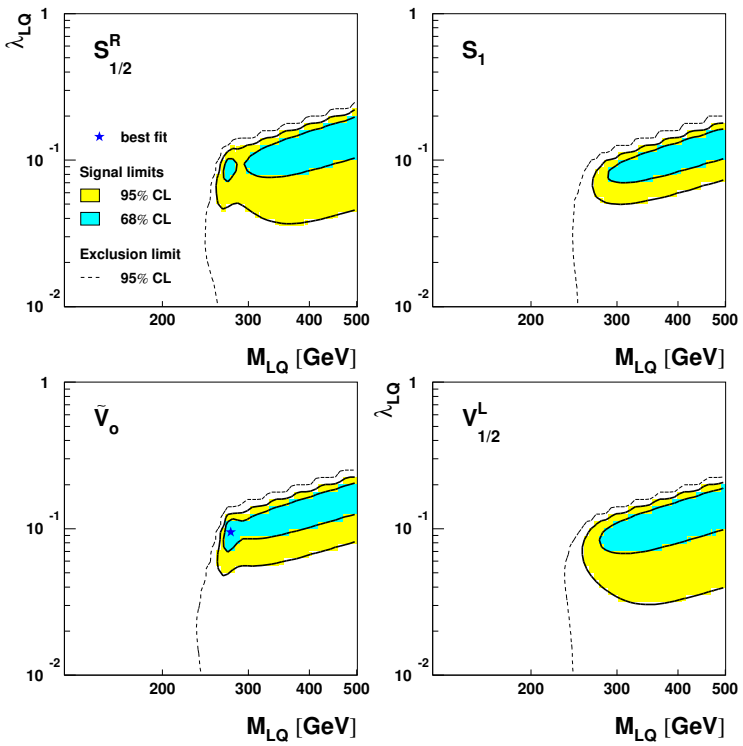

Figure 1: Signal limits on 68% and 95% CL for different leptoquark models (as indicated in the plot) resulting from the global analysis of existing data [1]. Dashed lines indicate the 95% CL exclusion limits. For $\tilde{V}_o$ model a star indicates the best fit parameters. For other models the best fit is obtained in the contact interaction limit $M_{LQ} \to \infty$. For $S_{1/2}$ and $V_{1/2}$ models, the superscript indicates the considered chirality of the Yukawa coupling.

slight violation of the CKM matrix unitarity and HERA high-Q^2 results. Existence of leptoquark state with mass of 300–400 GeV and Yukawa coupling of the order of $0.3e$ could explain these effects.

4 Leptoquark production at TESLA

Taking into account existing experimental constraints it is rather unlikely that leptoquarks have masses below 250 GeV, so they can be pair produced at TESLA at $\sqrt{s} = 500$ GeV. Therefore, only the high energy TESLA running option is considered in this paper, with $\sqrt{s} = 800$ GeV and expected integrated luminosity $\mathcal{L} = 500$ fb^{-1}.

In e^+e^- annihilation, leptoquarks can be pair-produced via photon and Z boson s-channel exchange and via t-channel exchange of quarks, as shown in Figure 2. Contribution from γ and Z exchange is determined by the leptoquark type: its spin, charge and weak isospin. Only the process with the t-channel quark exchange is sensitive to the leptoquark-electron-quark Yukawa coupling. The value of the Yukawa coupling influences both the

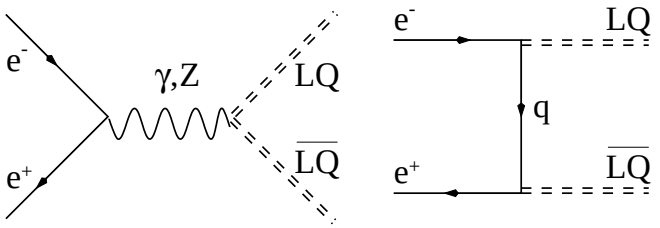

Figure 2: Diagrams for leptoquark pair production in e^+e^- collisions.

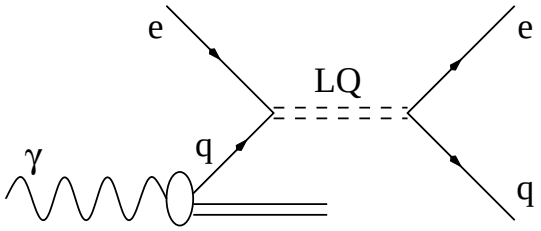

Figure 3: Diagram for single leptoquark production in $e^{\pm}\gamma$ collisions.

total pair production cross-section value[2] as well as the angular distribution of the produced leptoquark pairs. Analysis of the leptoquark pair production presented in this paper is based on the formulae and prescriptions given in [10] and implemented in the LQPAIR program [11][3].

High energy e^+e^- collisions can be also used to study single leptoquark production in $e^{\pm}\gamma$ collisions. Considered in this paper are $e^{\pm}\gamma$ collisions resulting from the effective electron and positron photon flux, described by the Weizsäcker-Williams Approximation (WWA), and from the electron and positron beam beamstrahlung, as simulated by CIRCE [12]. It is assumed that the leptoquark is produced in the electron fusion with a quark inside the photon,[4] as shown in Figure 3 and implemented in PYTHIA [14].

In addition to the leptoquark production, following background processes has been generated with PYTHIA version 6.152:

- Z-pair production: $e^+e^- \to Z^\circ Z^\circ$,
- W-pair production: $e^+e^- \to W^+W^-$,
- top quark pair production: $e^+e^- \to t\bar{t}$,
- other ("light") fermion pair production: $e^+e^- \to f\bar{f}$, $(f \neq t)$,
- Neutral Current $e^{\pm}\gamma$ deep inelastic scattering (NC DIS): $e^{\pm}\gamma \to e^{\pm}X$.

[2]Because of the interference with the s-channel γ and Z exchange, t-channel quark exchange can increase or decrease the total leptoquark pair production cross-section.

[3]Generation of the leptoquark decay angles in LQPAIR has been corrected.

[4]An alternative approach is to consider direct process $e\gamma \to LQ\ q$ [13]. Both approaches give very similar results [3].

Generated process	$\sigma_{e^+e^-}$ [fb]	Generated events	Luminosity [fb^{-1}]
$e^+e^- \to^{-5/3} S_{1/2}\,^{+5/3}\bar{S}_{1/2}$	27.0	13485	500
$e^+e^- \to^{-2/3} S_{1/2}\,^{+2/3}\bar{S}_{1/2}$	11.6	28963	2500
$e^+e^- \to^{-1/3} S_\circ\,^{+1/3}\bar{S}_\circ$	1.11	11110	10000
$e^+e^- \to^{-4/3} S_1\,^{+4/3}\bar{S}_1$	28.2	14100	500
$e^+e^- \to^{-1/3} S_1\,^{+1/3}\bar{S}_1$	1.11	11110	10000
$e^\pm\gamma \to^{\pm 1/3} S_\circ\, X$	1.92	10000	5200
$e^+e^- \to Z^\circ Z^\circ$	313	240000	766
$e^+e^- \to W^+W^-$	4320	657000	152
$e^+e^- \to t\bar{t}$	306	192000	628
$e^+e^- \to f\bar{f}\ (f \neq t)$	6860	960000	140
$e^\pm\gamma \to e^\pm X$	2060	400000	194

Table 2: Cross-section values, numbers of generated Monte Carlo events and effective Monte Carlo luminosities, for different processes considered in this paper. All background samples used in the analysis are shown, but only selected signal samples. Signal samples were generated for leptoquark mass M=350 GeV, $\lambda_L = \lambda_R = 0$ for pair production or $\lambda_L = 0$ and $\lambda_R = 0.1$ e for single leptoquark production. Background from $e^\pm\gamma$ NC DIS was generated with cut on electron-quark invariant mass $M_{eq} > 300$ GeV. Cross-sections are given for e^+e^- scattering at $\sqrt{s} = 800$ GeV, including beamstrahlung and radiative corrections.

Cross-section values for selected signal and background samples, numbers of generated Monte Carlo events and effective Monte Carlo luminosities are summarized in Table 2. When generating signal and background events, radiative effects were taken into account in both LQPAIR and PYTHIA. Incoming beams energies were smeared using CIRCE package (version 5, revision 1998 05 05) [12]. Parton showering and hadronisation was done with JETSET. Detector response was simulated using a parametric Monte Carlo program SIMDET (version 3.01) [15]. Energy flow algorithm implemented in SIMDET was used to join tracker and calorimeter information. Durham jet finding algorithm was then used to group energy flow objects (corresponding, in most cases, to single particles) into given number of clusters.

5 Event selection

Three leptoquark production and decay channels were considered in this analysis:

- pair-production, with both leptoquarks decaying to $e^\pm$ and jet ($eejj$ events),
- pair-production, with one leptoquark decaying to $e^\pm$ and jet and the other one to neutrino and jet ($e\nu jj$ events),

- single-production, with leptoquark decaying to $e^{\pm}$ and jet ($ej(j)$ events).

For all channels, event selection cuts were introduced to suppress background from other processes and allow good event reconstruction. Selection algorithms were optimized for reconstruction of leptoquark production events with M_{LQ}=350 GeV.

5.1 Selection of $eejj$ events

Cuts used to select leptoquark pair-production candidate events, with both leptoquarks decaying into electron (positron) and jet:

$$e^+e^- \;\rightarrow\; LQ\,\overline{LQ} \;\rightarrow\; eejj$$

- Pre-selection cuts:
  - total energy E of an event: $E > 0.9\sqrt{s}$,
  - total transverse energy E_t of an event: $E_t > 0.4\sqrt{s}$,
  - total transverse momentum p_t to E_t ratio: $p_t/E_t < 0.1$,
- Four energy clusters, with transverse momenta $p_t^i > 20$ GeV, are reconstructed using the Durham jet algorithm (y_{cut} not constrained):
  - two clusters are identified as an isolated electron and positron,
  - two clusters are identified as high multiplicity ($N_p \geq 5$) jets.
- Z-pair background rejection.
  Rejected are events fulfilling any of the following conditions:
  - invariant mass of the e^+e^- system $80 < M_{ee} < 100$ GeV,
  - invariant mass of the two jet system $70 < M_{jj} < 100$ GeV,
  - sum of two masses $M_{ee} + M_{jj} < 200$ GeV.
- difference between reconstructed masses of leptoquark (e^--jet) and anti-leptoquark (e^+-jet): $\Delta M_{ej} < 60$ GeV,
- difference between leptoquark and anti-leptoquark azimuthal angle[5]: $|\Delta\phi - \pi| < 0.15$,
- reconstructed mass within $\pm$ 25 GeV from the nominal value.

Expected signal and background event distributions in the main selection variables and in the reconstructed leptoquark production angle are presented in Figure 4. The selection efficiency for scalar and vector leptoquark pair-production, for leptoquark mass $M_{LQ} = 350$ GeV and $\sqrt{s} = 800$ GeV, is about 50%. Estimated background from Z-pair production[6] corresponds to the cross-section of about 0.015 fb (7 events in 500 fb^{-1}) and is considered to be negligible.

[5] Emission angle measured in the plane perpendicular to the beam axis.

[6] No other background Monte Carlo events survive the cuts

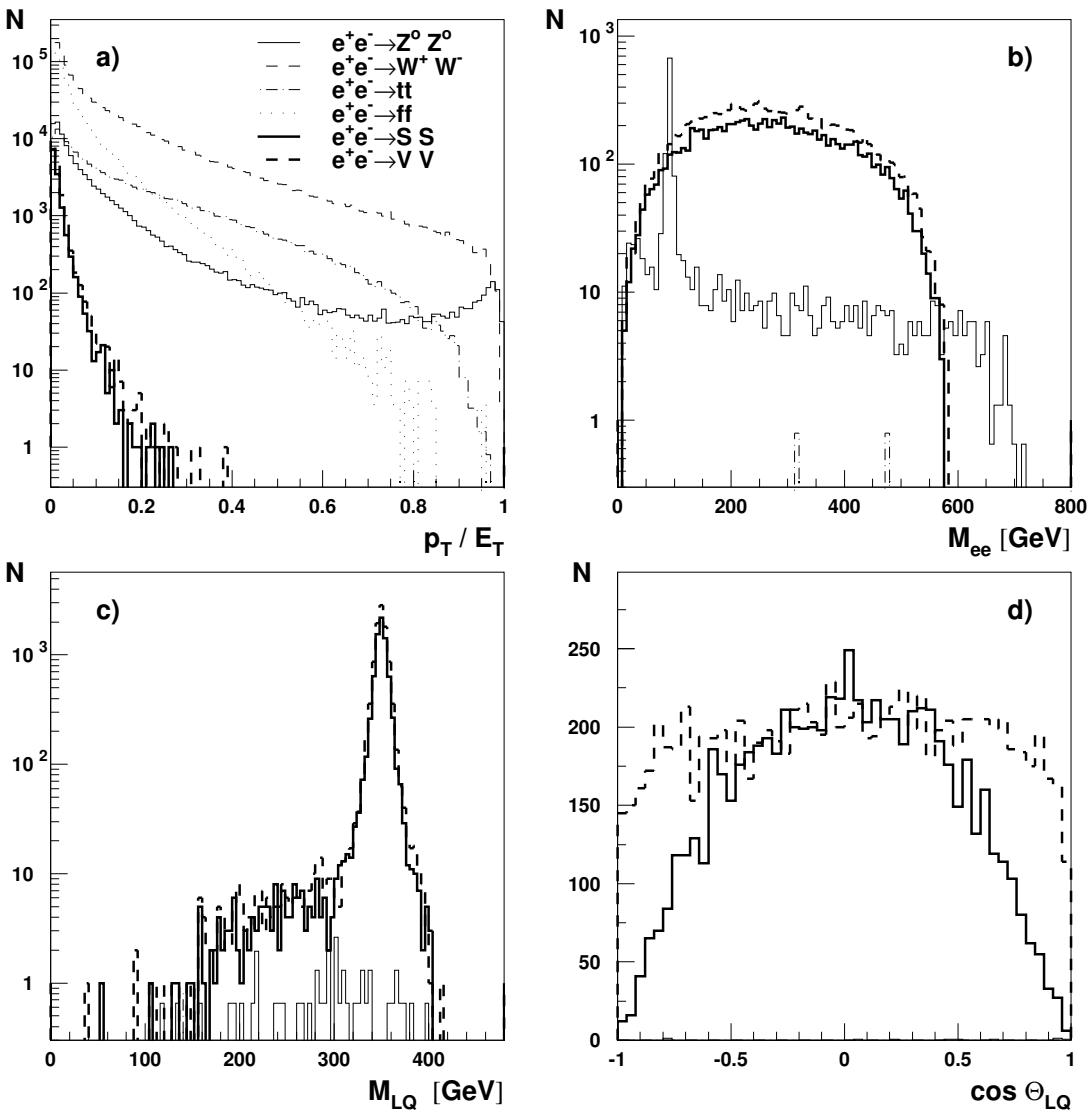

Figure 4: Selection of the leptoquark pair-production events in the $eejj$ channel. Distributions for signal (scalar $S_{1/2}$ or vector V_0 leptoquarks with M=350 GeV) and background events (Z° pair-production, $W^\pm$ pair-production, $t\bar{t}$ pair-production and production of other fermion pairs $f\bar{f}$ ($f \neq t$), as indicated in the plot), expected for the integrated luminosity of $500 fb^{-1}$, are shown for: ratio of the total transverse momentum to the transverse energy, before any selection cuts (a), invariant mass of the identified e^+e^- pair M_{ee}, after pre-selection and lepton identification cuts (b), reconstructed leptoquark mass M_{LQ}, after all selection cuts (c), leptoquark production angle Θ_{LQ}, in $\pm$ 25 GeV mass window (d).

5.2 Selection of $e\nu jj$ events

Main cuts used to select leptoquark pair-production candidate events, with one leptoquark decaying to electron (positron) and jet and the other one to neutrino and jet:

$$e^+e^- \;\rightarrow\; LQ\,\overline{LQ} \;\rightarrow\; e\nu jj$$

- Pre-selection cuts:
  - total transverse energy E_t of an event: $E_t > 0.25\sqrt{s}$,
  - total transverse momentum p_t to E_t ratio: $p_t/E_t > 0.1$,
  - total invariant mass M_{tot} of an event: $M_{tot} > 0.5\sqrt{s}$,
- Three energy clusters, with energy $100 < E_i < 300$ GeV and transverse momenta $p_t^i > 50$ GeV, are reconstructed using the Durham jet algorithm, with y_{cut}=0.006:
  - one cluster is identified as an isolated electron or positron,
  - two clusters are identified as high multiplicity ($N_p \geq 5$) jets.
- W-pair background rejection.
  Rejected are events fulfilling any of the following conditions:
  - invariant mass of the two jet system $M_{jj} < 110$ GeV,
  - reconstructed $e\nu$ invariant mass $M_{e\nu} < 150$ GeV,
  - sum of two masses $M_{jj} + M_{e\nu} < 350$,
- difference between mass of the (anti-)leptoquark reconstructed from electron-jet and neutrino-jet final state, $-80 < M_{ej} - M_{\nu j} < 50$ GeV,
- lepton emission angle in the (anti-)leptoquark rest frame $\cos\theta_l^\star > -0.7$,
- mass reconstructed from electron-jet final state M_{ej} within ± 20 GeV from the nominal value.

Expected signal and background event distributions in the main selection variables and in the reconstructed leptoquark production angle are presented in Figure 5. The selection efficiency for scalar and vector leptoquark pair-production, for leptoquark mass $M_{LQ} = 350$ GeV and $\sqrt{s} = 800$ GeV, is about 30%. Estimated background from $W^\pm$ and $t\bar{t}$ pair-production corresponds to the cross-section of about 0.13 fb (65 events for 500 fb^{-1}) and is taken into account in the presented analysis.

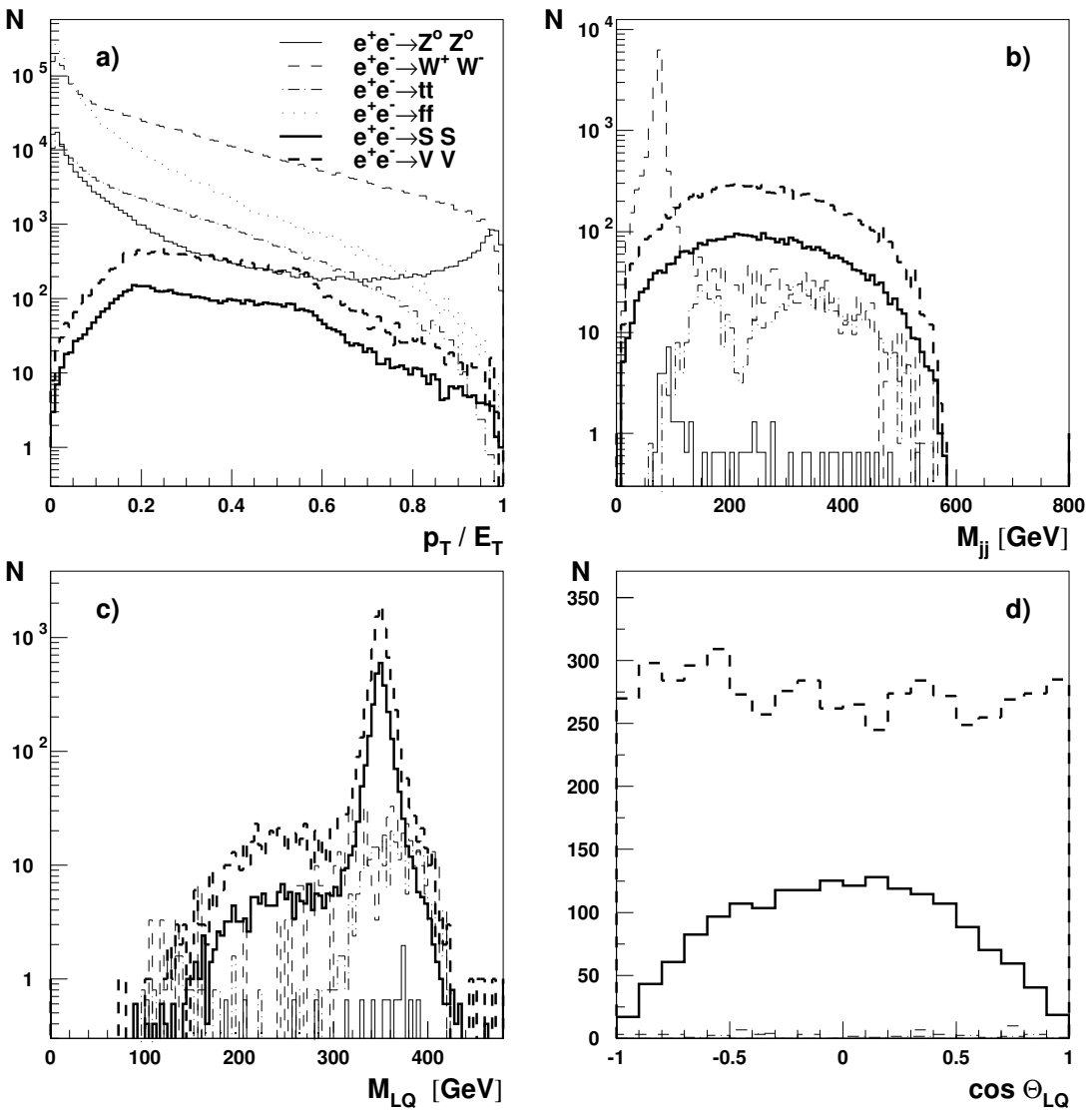

Figure 5: Selection of the leptoquark pair-production events in the $e\nu jj$ channel. Distributions for signal (scalar $S_{1/2}$ or vector V_0 leptoquarks with M=350 GeV) and background events (Z° pair-production, $W^\pm$ pair-production, $t\bar{t}$ pair-production and production of other fermion pairs $f\bar{f}$ ($f \neq t$), as indicated in the plot), expected for the integrated luminosity of $500 fb^{-1}$, are shown for: ratio of the total transverse momentum to the transverse energy, before any selection cuts (a), invariant mass of the jet system M_{jj}, after pre-selection and lepton identification cuts (b), reconstructed leptoquark mass M_{LQ}, after all selection cuts (c), leptoquark production angle Θ_{LQ}, in $\pm$ 20 GeV mass window (d).

5.3 Selection of $ej(j)$ events

Leptoquarks can be also single-produced at TESLA, in $e^{\pm}\gamma$ collisions:

$$\gamma e^{-} \;\rightarrow\; LQ + X \;\rightarrow\; ej + X$$

where X is the "photon remnant": hadronic state remaining after leptoquark production in electron-quark fusion. Reconstruction of the remnant jet turns out to be very important for efficient leptoquark selection and background reduction. Direction of the remnant production gives an independent tag on the charge of the scattered $e^{\pm}$, strongly suppressing background from NC $e^{\pm}\gamma$ DIS event with wrong reconstruction of the scattered lepton charge.

Cuts used to select single leptoquark production events:

- Pre-selection cuts:
  - total energy E of an event: $E > 0.5\sqrt{s}$,
  - total transverse energy E_t of an event: $E_t > 50$ GeV,
  - total transverse momentum p_t to E_t ratio: $p_t/E_t < 0.1$,
  - total invariant mass M_{tot} of an event: $300 < M_{tot} < 600$ GeV,
- Three energy clusters are reconstructed using the Durham jet algorithm (without constraining y_{cut}). These clusters are identified as:
  - an isolated electron or positron with transverse momentum $p_t^e > 80$ GeV,
  - hadronic jet from leptoquark decay with transverse momentum $p_t^j > 80$ GeV,
  - photon remnant with transverse momentum $p_t^r < 50$ GeV and $p_t^r < 0.1\ p_t^j$; remnant emission angle w.r.t. the photon direction $\cos\theta > 0.8$.
- mass reconstructed from decay electron energy and direction[7] M_e within $\pm$ 8 GeV from the nominal value.

Expected signal and background event distributions in the selected variables are presented in Figure 6. The selection efficiency for scalar leptoquark production, for leptoquark mass $M_{LQ} = 350$ GeV and $\sqrt{s} = 800$ GeV, is about 15%. Large, irreducible background comes from $e^{\pm}\gamma$ NC DIS. However, NC DIS background results in the steeply falling distribution of the electron emission angle in the leptoquark rest frame $\theta_e^{\star}$, whereas for scalar leptoquark production the distribution is flat at high $\theta_e^{\star}$ (see Figure 6d). Estimated background from remaining processes is about 8 event (in the selected mass window), mainly from W-pair production, and is taken into account.

[7] For high electron scattering angles, leptoquark mass resolution for "electron" method (from electron energy and scattering angle only; using incident beam energy) is better than from electron-jet invariant mass (about 4 GeV and 6 GeV respectively).

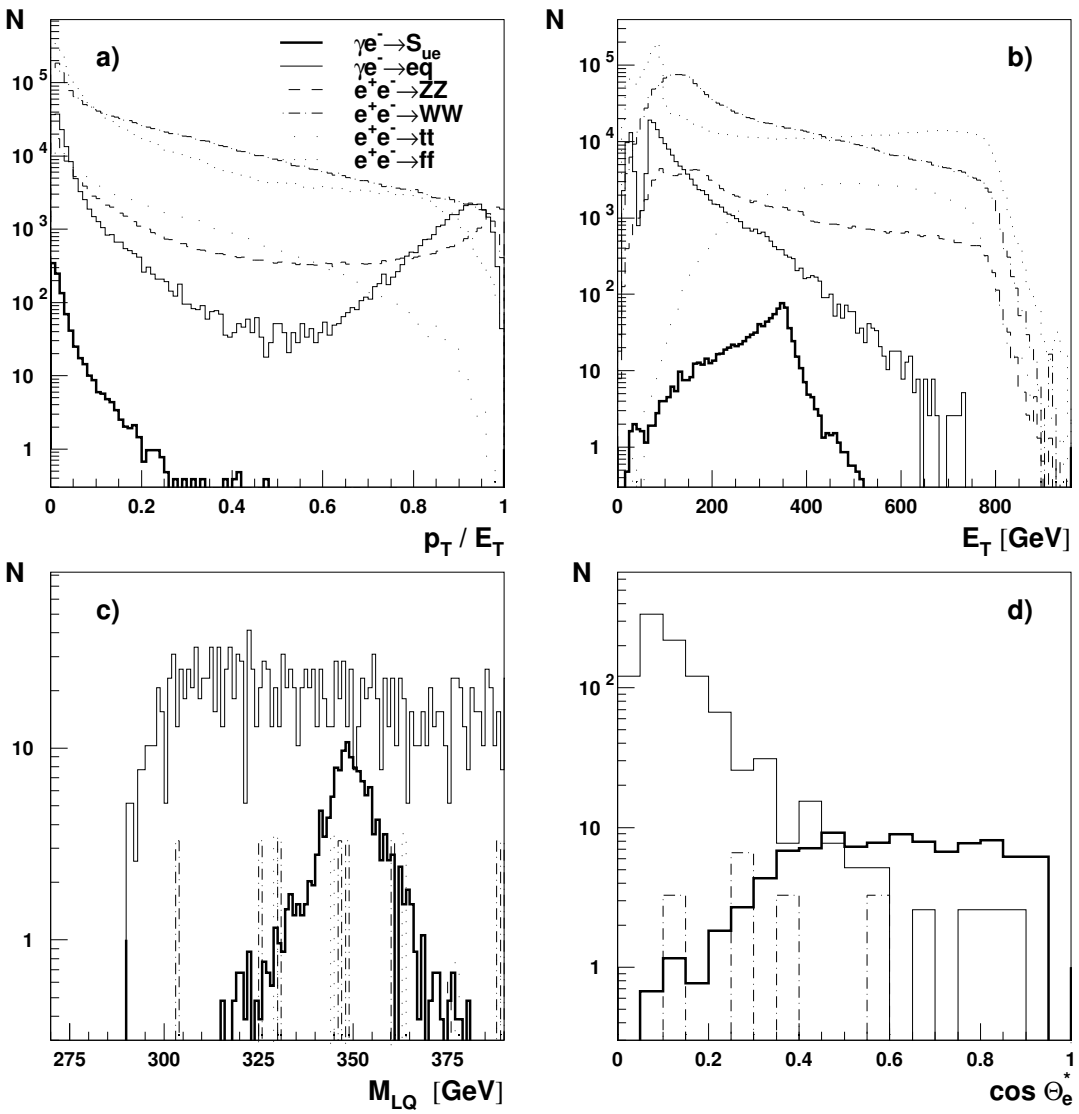

Figure 6: Selection of the single leptoquark production events ($ej(j)$ channel). Distributions for signal (scalar S_o^R leptoquark with M=350 GeV and $\lambda_R = 0.1$ e) and background events ($e^{\pm}\gamma$ NC DIS with electron-quark invariant mass $M_{eq} > 300$ GeV, Z° pair-production, $W^{\pm}$ pair-production, $t\bar{t}$ pair-production and production of other fermion pairs $f\bar{f}$ ($f \neq t$), as indicated in the plot), expected for the integrated e^+e^- luminosity of $500 fb^{-1}$, are shown for: ratio of the total transverse momentum to the transverse energy, before any selection cuts (a), the total transverse energy, before any selection cuts (b), reconstructed leptoquark mass M_{LQ}, after all selection cuts (c), electron emission angle in the leptoquark rest frame $\theta_e^\star$, in $\pm$ 8 GeV mass window (d).

6 Determination of the Yukawa couplings

Considered in this note is the possibility of the leptoquark Yukawa coupling measurement from the observed angular leptoquark distributions. Three distributions are considered: leptoquark production angle distribution in the pair-production process, in $eejj$ channel and in $e\nu jj$ channel, and the decay electron emission angle in the single leptoquark production process ($ej(j)$ channel). Yukawa coupling determination has been studied for three leptoquark types: $S_\circ$ (iso-singlet), $S_{1/2}$ (iso-doublet) and S_1 (iso-triplet). For $S_\circ$ and $S_{1/2}$ leptoquarks both left-handed and right-handed Yukawa couplings (λ_L and λ_R) are considered, whereas S_1 leptoquark couples only to left-handed leptons.

Observed angular distributions, in three considered channels, for $S_\circ^L$ leptoquark production are presented in Figure 7. Events were generated assuming M_{LQ} =350GeV and λ_L=0.15e (λ_R=0). Numbers of observed events shown on the plots correspond to the integrated luminosity of 500 fb^{-1}. Result of the simultaneous log-likelihood fit to the three distributions is indicated by the solid line. Precision of the coupling determination, for the assumed parameter values is about 6%. This high precision results mainly from the measurement of the single leptoquark production process. However, single leptoquark production does not distinguish between left- and right-handed Yukawa couplings. Measurement of other distributions, related to the leptoquark pair-production, is required to verify the chirality of the coupling. This is demonstrated in Figure 8. 2σ ($\Delta \ln \mathcal{L} = 2$) contours in (λ_L, λ_R), resulting from the two parameter fits to the separate distributions are compared with 1σ ($\Delta \ln \mathcal{L} = 0.5$) and 2σ contours from the simultaneous fit to the three distributions, as show in Figure 7. Using information from both single leptoquark production and pair-production λ_L and λ_R can be simultaneously constrained. The value of the leptoquark Yukawa coupling can be precisely determined and its chirality unambiguously defined.

Measurement of the Yukawa couplings for $S_\circ$ would be the most difficult one at TESLA, as $S_\circ$ pair-production cross-section is the smallest. Much better measurement is possible for $S_{1/2}$ and S_1 leptoquarks. Corresponding results are shown in Figures 9 and 10 (for $S_{1/2}^R$, assuming λ_R=0.15e), and in Figures 11 and 12 (for S_1, assuming λ_L=0.15e). Presented results confirm that precise determination of the Yukawa couplings at TESLA will be possible even in the domain, which will not be accessible at LHC.[8]

Precision of the leptoquark Yukawa coupling determination, for different scalar leptoquark models, has been also studied as a function of the coupling value (for leptoquark mass M_{LQ}=350 GeV) and as a function of the leptoquark mass (for fixed value of coupling: λ_L=0.15e or λ_R=0.15e). Results are shown in Figures 13 and 14 respectively. Determination of the leptoquark Yukawa coupling, seems to be possible down to the coupling values or about 0.05e. Precision of the measurement very slowly deteriorates with the increasing leptoquark mass (for masses up to 390 GeV), as it results mainly from the single lepto-

[8]Coupling values chosen are just below the expected exclusion limits from Drell-Yan electron pair-production at LHC, with 100 fb^{-1} [3].

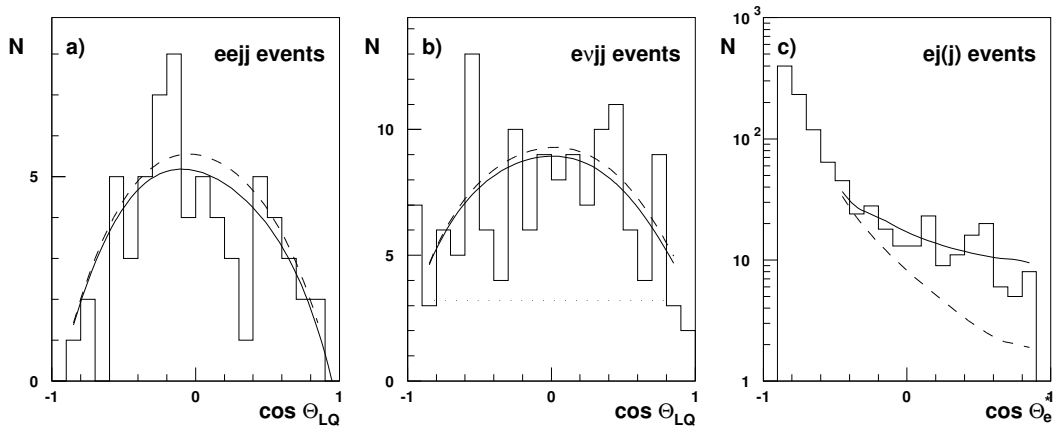

Figure 7: Angular distributions used to determine Yukawa couplings of the $S_\circ^L$ leptoquark: leptoquark production angle in the pair-production process, reconstructed in the $eejj$ channel (a), leptoquark production angle reconstructed in the $e\nu jj$ channel (b) and the decay electron emission angle in the leptoquark rest frame, for the single leptoquark production process (c). Leptoquark production events were generated assuming M_{LQ} =350GeV and λ_L=0.15e (λ_R=0). Solid lines represent the result of the simultaneous log-likelihood fit to the three distributions. Dashed line indicates model expectations for $\lambda_L \to 0$. Dotted line shows the expected background from $W^\pm$ and $t\bar{t}$ pair production (b).

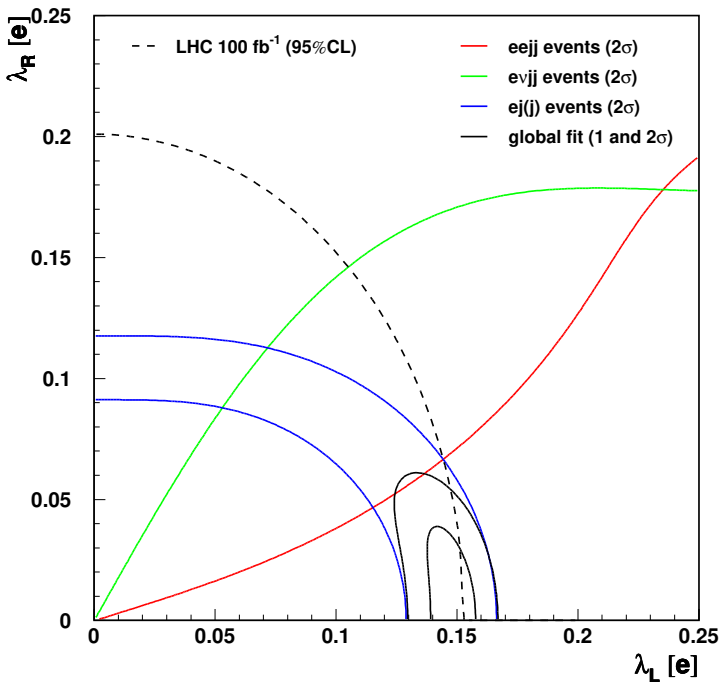

Figure 8: Results of the log-likelihood fit to the $S_\circ^L$ leptoquark angular distributions shown in Figure 7. 2σ ($\Delta \ln \mathcal{L} = 2$) contours in (λ_L, λ_R), resulting from the fits to the separate distributions (as indicated in the plot) are compared with 1σ ($\Delta \ln \mathcal{L} = 0.5$) and 2σ contours from the simultaneous fit to the three distributions. Also shown are 95% CL exclusion limits expected from the Drell-Yan e^+e^- pair-production at the LHC. Leptoquark production events were generated assuming M_{LQ} =350GeV and λ_L=0.15e (λ_R=0). Luminosity uncertainty is 1%.

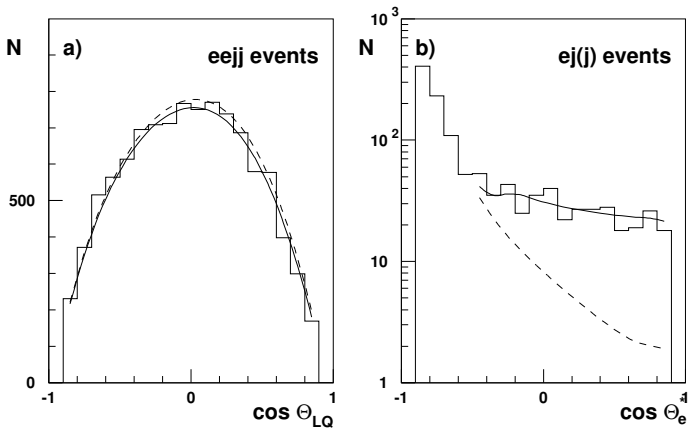

Figure 9: Angular distributions used to determine Yukawa couplings of the $S^R_{1/2}$ leptoquark: leptoquark production angle in the pair-production process, reconstructed in the $eejj$ channel (a) and the decay electron emission angle in the leptoquark rest frame, for the single leptoquark production process (b). Leptoquark production events were generated assuming M_{LQ} =350GeV and λ_R=0.15e (λ_L=0). Solid lines represent the result of the simultaneous log-likelihood fit to the three distributions. Dashed line indicates model expectations for $\lambda_R \to 0$.

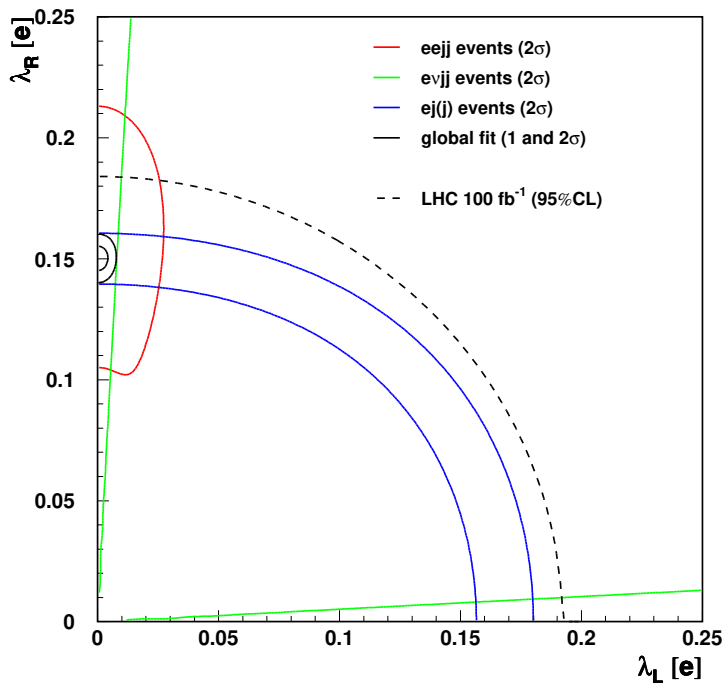

Figure 10: Results of the log-likelihood fit to the $S^R_{1/2}$ leptoquark angular distributions shown in Figure 9. 2σ ($\Delta \ln \mathcal{L} = 2$) contours in (λ_L, λ_R), resulting from the fits to the separate distributions (as indicated in the plot) are compared with 1σ ($\Delta \ln \mathcal{L} = 0.5$) and 2σ contours from the simultaneous fit to the three distributions. Also shown are 95% CL exclusion limits expected from the Drell-Yan e^+e^- pair-production at the LHC. Leptoquark production events were generated assuming M_{LQ} =350GeV and λ_R=0.15e (λ_L=0). Luminosity uncertainty is 1%.

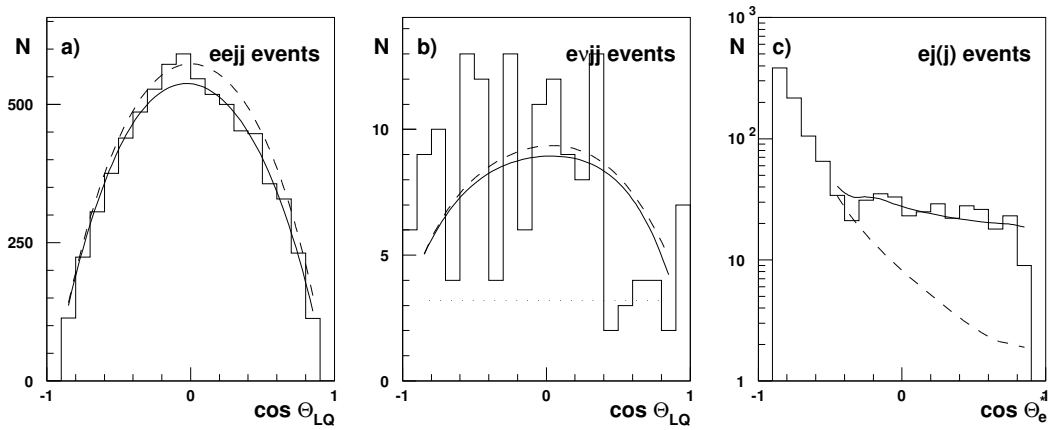

Figure 11: Angular distributions used to determine Yukawa couplings of the S_1 leptoquark: leptoquark production angle in the pair-production process, reconstructed in the $eejj$ channel (a), leptoquark production angle reconstructed in the $e\nu jj$ channel (b) and the decay electron emission angle in the leptoquark rest frame, for the single leptoquark production process (c). Leptoquark production events were generated assuming M_{LQ} =350GeV and λ_L=0.15e. Solid lines represent the result of the simultaneous log-likelihood fit to the three distributions. Dashed line indicates model expectations for $\lambda_L \to 0$. Dotted line indicates the expected background from $W^{\pm}$ and $t\bar{t}$ pair production (b).

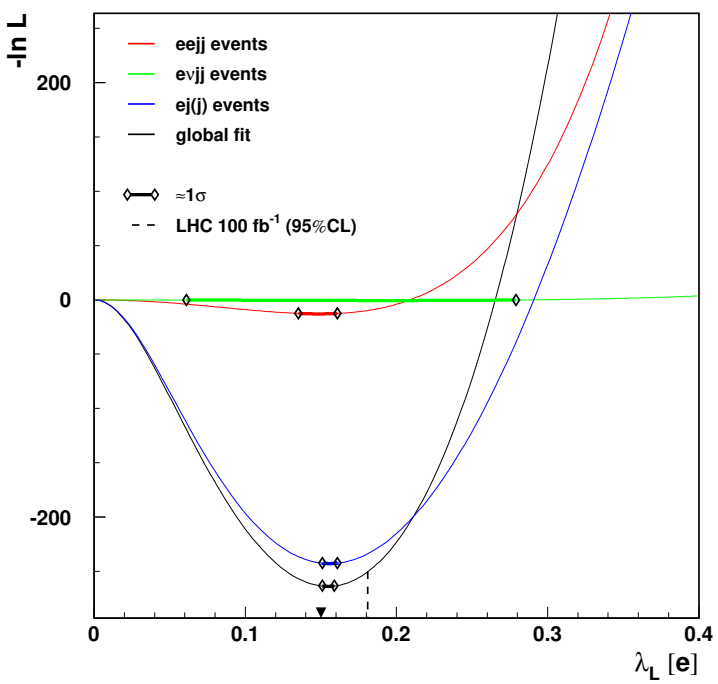

Figure 12: Log-likelihood curve ($-\ln \mathcal{L}$) for S_1 leptoquark, resulting from the fits of separate angular distributions and from the simultaneous fit to the three distributions, as indicated in the plot. Thicker lines indicate $\pm$ 1σ ($\Delta \ln \mathcal{L}$ = 0.5) errors on λ_L, resulting from the fits. Also shown are 95% CL exclusion limit expected from the Drell-Yan e^+e^- pair-production at the LHC. Leptoquark production events were generated assuming M_{LQ} =350GeV and λ_L=0.15e. Luminosity uncertainty is 1%.

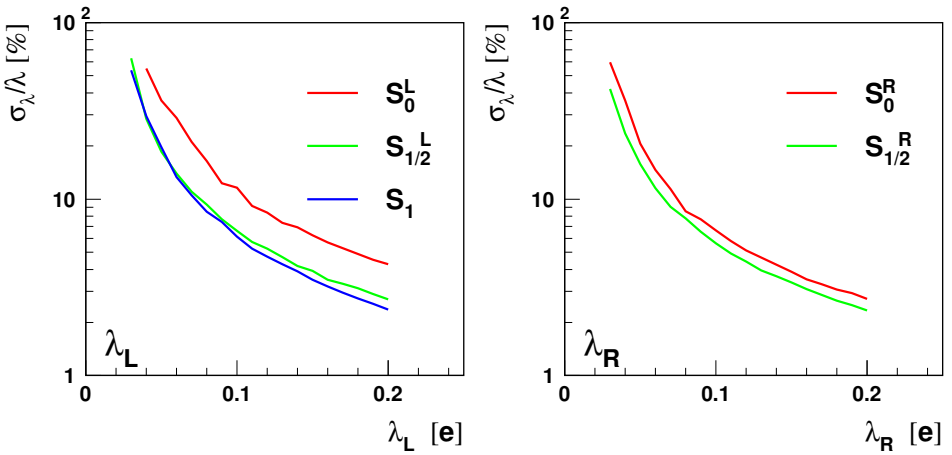

Figure 13: Relative precision of the leptoquark Yukawa coupling determination, for left- (left plot) and right-handed (right plot) couplings, for indicated leptoquark models. Expected result of the simultaneous log-likelihood fit to the three considered distributions, for M_{LQ} =350GeV, as a function of the coupling value.

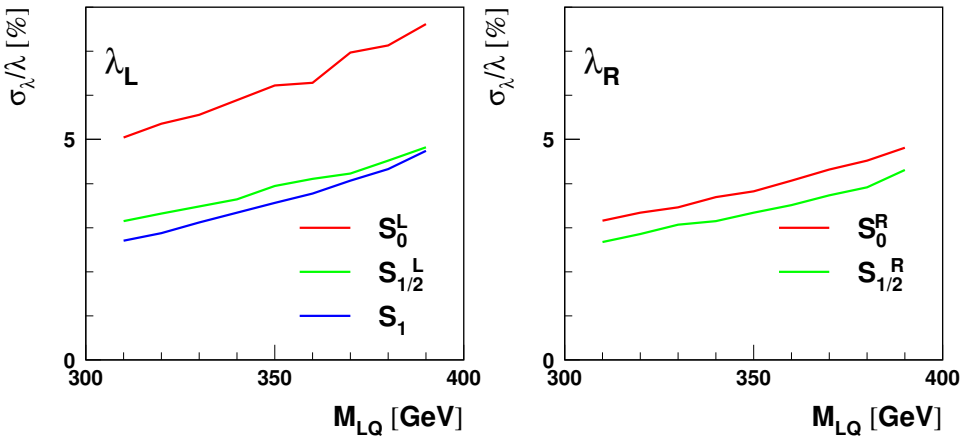

Figure 14: Relative precision of the leptoquark Yukawa coupling determination, for indicated leptoquark models. Expected result of the simultaneous log-likelihood fit to the three considered distributions, for λ_L=0.15e (left plot) and λ_R=0.15e (right plot), as a function of the leptoquark mass.

quark production measurements. Shown in Figures 15 are 1σ and 2σ contours in (λ_L, λ_R), for $S_{1/2}$ leptoquark with λ_L=0.15e or λ_R=0.15e, for leptoquark mass M_{LQ} =330, 350, 370 and 390 GeV. Measurement of the leptoquark pair-production process will allow to distinguish between left- and right-handed Yukawa couplings even for leptoquark masses very close to the pair-production kinematic limit.

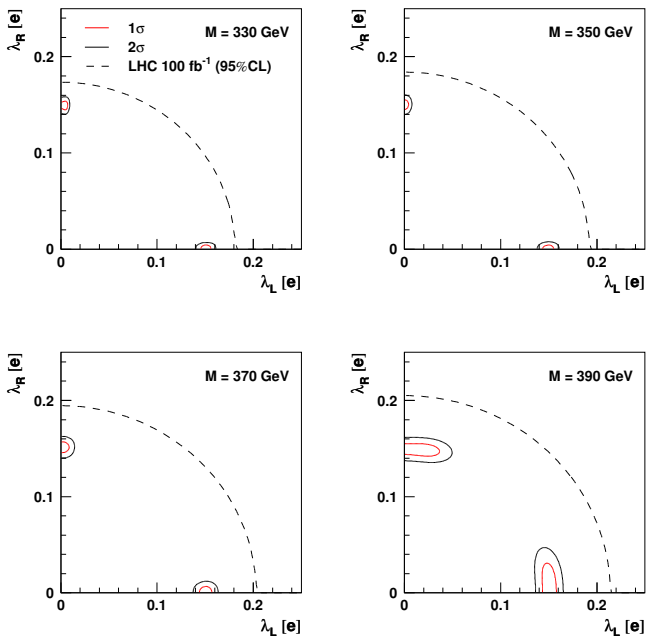

Figure 15: Results of the log-likelihood fit to the $S_{1/2}$ leptoquark angular distributions. 1σ and 2σ contours in (λ_L, λ_R), resulting from the simultaneous fit to all considered distributions are compared for different leptoquark masses, as indicated in the plot. Also shown are 95% CL exclusion limits expected from the Drell-Yan e^+e^- pair-production at the LHC. Leptoquark production events were generated assuming λ_L=0.15e or λ_R=0.15e. Luminosity uncertainty is 1%.

7 Summary

Measurement of the Yukawa couplings of the first-generation leptoquarks has been studied for e^+e^- collisions at TESLA, at $\sqrt{s}$ =800 GeV. By combining measurements from different production and decay channels, determination of Yukawa couplings with precision on the few per-cent level is possible. TESLA will be sensitive to very small leptoquark Yukawa couplings not accessible at LHC, down to $\lambda_{L,R} \sim 0.05e$. Distinction between left-handed and right-handed Yukawa couplings is feasible even for leptoquark masses very close to the pair-production kinematic limit.

TESLA sensitivity to very small Yukawa couplings is limited mainly by the statistics of single leptoquark production events. In e^+e^- running mode of TESLA, considered in this paper, single leptoquark production is suppressed by a very small flux of high energy bremsstrahlung and beamstrahlung photons. If TESLA collider is run in $e\gamma$ mode, cross-section for single leptoquark production will increase significantly and much smaller Yukawa couplings can be searched for.

References

[1] A.F.Żarnecki, Euro. Phys. J. **C17** (2000) 695.

[2] S.Abdullin, F.Charles, F.Luckel, CMS Note 1999/027.

[3] A.F.Żarnecki, hep-ph/0006335.

[4] W.Buchmüller, R.Rückl and D.Wyler, Phys. Lett. **B191** (1987) 442;
Erratum: Phys. Lett. **B448** (1999) 320.

[5] A.Djouadi, T.Köhler, M.Spira, J.Tutas, Z. Phys. **C46** (1990) 679.

[6] W.Buchmüller and D.Wyler, Phys. Lett. **B177** (1986) 377.

[7] J.Kalinowski, R.Rückl, H.Spiesberger and P.M.Zerwas, Z. Phys. **C74** (1997) 595.

[8] S.C.Bennett and C.E.Wieman, Phys. Rev. Lett. **82** (1999) 2484.

[9] LEP Electroweak Working Group, C.Geweniger *et al*, LEP2FF/00-01.

[10] R.Rückl, R.Settles and H.Spiesberger, hep-ph/9709315.

[11] H.Spiesberger, *LQPAIR version 2.03 - A Monte Carlo Generator for Leptoquark Pair Production in e^+e^- Annihilation*, October 1996,
`http://www.desy.de/~hspiesb/lqpair.html`.

[12] T.Ohl, *CIRCE version 1.31*
T.Ohl, hep-ph/9607454.

[13] F.Cuypers, hep-ph/9508397.

[14] T. Sjostrand, *PYTHIA version 6.152*, `http://www.thep.lu.se/~torbjorn/Pythia.html`
T. Sjostrand, Computer Physics Commun. 82 (1994) 74.

[15] M.Pohl, H.J.Schreiber, DEYS 99-030.